

Article ID: 1007-8827(2006)04-0315-06

Kinetics of the thermal decomposition of intercalation compounds during exfoliation

REN Hui^{1,2}, KANG Fei-yu¹, JIAO Qing-jie², CUI Qing-zhong²

(1. Graduate School at Shenzhen, Tsinghua University, Shenzhen 518055, China;

2. National Key Laboratory of Explosion Science and Technology, Beijing Institute of Technology, Beijing 100081, China)

Abstract: The phase transformations and thermal decomposition of the following graphite intercalation compounds (GICs), $\text{HNO}_3\text{-CH}_3\text{COOH-GIC}$, $\text{H}_2\text{SO}_4\text{-GIC}$ and $\text{H}_2\text{SO}_4\text{-CH}_3\text{COOH-GIC}$, were measured by an FTIR-associated TG apparatus. Using Kissinger and Ozawa principles, the kinetic parameters of some typical exfoliation reactions were evaluated and the thermal decomposition mechanism of the exfoliation process was determined. When the heating rate was in the range of 20–80 °C/min, the activation energies of the exfoliation reactions were all less than 120 kJ/mol.

Keywords: Exfoliation; Thermal analysis; Kinetics; Intercalation

CLC number: TQ165 O643.12

Document code: A

1 Introduction

Expanded graphite is produced from graphite intercalation compounds that are subjected to a thermal shock^[1]. As the intercalated species is rapidly volatilized, a significant expansion of the material along the crystallographic c-axis occurs^[2,3]. When expanded graphite is used as fire extinguishers, electromagnetic shielding materials, and sealed gaskets, expanded volume and rate will directly influence its performance in these applications^[4-7]. Whether exfoliation might occur, depends on the raw materials, heating rate, particle size, and intercalated species^[8-10]. Studies indicated that intercalated graphite could not expand with frame heating or electric cooker heating when its size was smaller than 88 μm ^[11,12]. With laser heating method with a heating rate as high as 10⁴ °C/s, the exfoliation of intercalated graphite is remarkable. Study on kinetics and phase transformation in the expanding process is very important for obtaining information on structural control and properties of expanded graphite. However, because volume expansions are usually higher than 200 g/mL and sample pool is very limited, it is difficult to carry out thermal analysis of expanded graphite using DSC and TG. Up to date, only few reports have been published on thermal analysis of expanded graphite.

In this article, fundamentals of chemical dynamics about exfoliation of graphite intercalation compounds are discussed. The phase transformation and

thermal decomposition were measured in situ with a FTIR-associated TG apparatus. Moreover, according to Kissinger and Ozawa principles, activation energy and exponent factor of exfoliation reaction were obtained from data tested under different heating rates.

2 Experimental

2.1 Apparatus and testing conditions

Thermogravimetric apparatus (Pyris-TGA, Perkin-Elmer Corp.) with a sensitivity of 10⁻⁸ g was employed to measure the change in thermo-flux by no more than microwatt in one minute.

Fourier transform infrared spectrometer (FTIR, Spectrum GX, Perkin-Elmer Corp.) with resolution of 0.1 cm⁻¹ and signal-to-noise ratio over 9 000:1 was employed to analyze the infrared spectra of the decomposed products collected, from which the decomposed products and their concentrations were obtained and decomposition mechanism was deduced.

In this study, phase transformation and thermal decomposition of three expandable graphite intercalation compounds ($\text{H}_2\text{SO}_4\text{-GIC}$, $\text{HNO}_3\text{-CH}_3\text{COOH-GIC}$, and $\text{H}_2\text{SO}_4\text{-CH}_3\text{COOH-GIC}$ ^[13-15]) were in situ measured by the FTIR-associated TG apparatus. The mass of each sample was lower than 7 mg under nitrogen atmosphere. Experimental temperature was changed from 25 °C to 600 °C with different heating rates of 20, 40, 60, and 80 °C/min.

Received date: 2006-05-26; **Revised date:** 2006-11-21

Foundation item: National Natural Science Foundation (50572047).

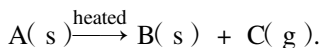
Corresponding author: KANG Fei-yu, E-mail: fykang@mail.tsinghua.edu.cn

Author introduction: REN Hui(1973-), female, Postdoctoral Candidate, engaged in research of nanometer function material.

E-mail: renhui@bit.edu.cn

2.2 Analysis theory

The exfoliation process is denoted as the formula:



The kinetics equation of reactions can be calculated with differential and integral forms. Kissinger arithmetic belongs to differential method^[16]. According to Arrhenius law, reaction rate can be written as:

$$\frac{d\alpha}{dt} = A \exp(-E/RT) f(\alpha), \quad (1)$$

where, α – reacted proportion after time, t ;

A – apparent exponential factor;

E – apparent activation energy, kJ/mol;

R – gas constant, $R = 8.314 \text{ J/mol} \cdot \text{K}$;

$f(\alpha)$ – differential form of dynamics mechanism function.

Suppose experimental temperature is raised steadily, substituting $f(\alpha) = (1 - \alpha)^n$ into equation (1) and by differential operation on either sides, equation (2) is obtained:

$$\frac{d}{dt} \left(\frac{d\alpha}{dt} \right) = \frac{d\alpha}{dt} \left[E \left(\frac{dT}{dt} \right) - An(1 - \alpha)^{n-1} \exp(-E/RT) \right]. \quad (2)$$

When temperature of reaction reach the highest temperature (T_p), $\frac{d}{dt} \left(\frac{d\alpha}{dt} \right) = 0$.

Suppose $n(1 - \alpha)^{n-1} e^{-E/RT_p}$ is independent of linear heating rate β and it is approximately equal to 1 in Kissinger equation^[17], equation (2) is rewritten as:

$$\frac{E\beta}{RT_p^2} = Ae^{-E/RT_p}. \quad (3)$$

Kissinger equation is obtained from logarithmic operation on either sides of equation (3):

$$\ln \left[\frac{\beta_i}{T_{pi}^2} \right] = \ln \frac{A_k R}{E_k} - \frac{E_k}{R} \frac{1}{T_{pi}}, \quad (4)$$

$i, k = 1, 2, 3, 4 \text{ (or } 5 \text{ and } 6).$

A line can be drawn when X-axis is $\frac{1}{T_{pi}}$ and Y-axis is

$\ln \left[\frac{\beta_i}{T_{pi}^2} \right]$. The apparent activation energy E_k and exponent factor A_k can be obtained from slope and intercept of this line.

Ozawa adopted integral operation. $G(\alpha)$ is represented by dynamics mechanism function and it can be related to $f(\alpha)$ as:

$$f(\alpha) = \frac{1}{G'(\alpha)} = \frac{1}{d[G(\alpha)]/d\alpha}. \quad (5)$$

Through approximate calculation, it is found that heating rate β , exponent factor A , and apparent activation energy E obeys the following equation:

$$\ln \beta = \lg \frac{AE}{RG(\alpha)} - 2.315 - 0.4567 \frac{E}{RT}. \quad (6)$$

Because the quantity that reacted is close to equivalency at peak temperature regardless of different heating rates, accurate solution of apparent activation energy is determined by Ozawa' law, which is based on the linear relationship between $\lg \beta$ and T^{-1} .

3 Results and discussion

Expandable graphite is a nonstoichiometric compound and its chemical structure cannot be determined. From Fig. 1, TG curves of H_2SO_4 -GICs are similar at different heating rates ranging from 40 to 80°C/min . When H_2SO_4 -GICs were heated, their TG curves started to decline slowly, indicating a gradual weight loss. From DTG curve, thermal decomposition of H_2SO_4 -GICs is divided into two steps. A small dehydration peak is located at temperature between 110 and 140°C with a weight loss of 1.7% – 2.0% . A significant weight loss began from around 250°C , where intercalated species decomposed to release radicals of SO_4^{2-} and H_2SO_4 . The total weight loss is 21% – 8% below 500°C .

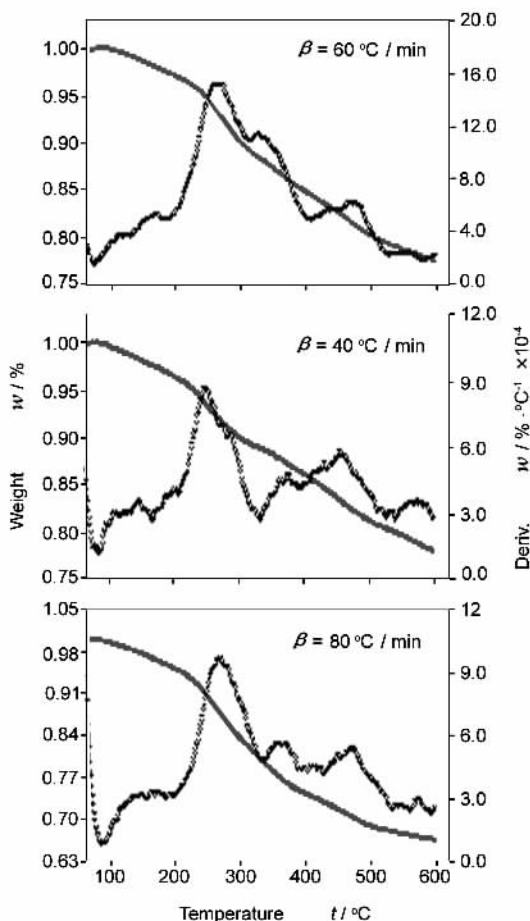


Fig. 1 TG and DTG curves of H_2SO_4 -GIC

To discuss exfoliation process of ternary graphite intercalation compounds, $\text{HNO}_3\text{-CH}_3\text{COOH-GIC}$ is regarded as research object to analyze thermal decomposition of two guest species. Fig. 2 shows TG and DTG curves of $\text{HNO}_3\text{-CH}_3\text{COOH-GIC}$ with a heating rate of $60\text{ }^\circ\text{C}/\text{min}$. The weight loss of $\text{HNO}_3\text{-CH}_3\text{COOH-GIC}$ mainly occurs between 220 and $350\text{ }^\circ\text{C}$, and the second decomposition peak is more evident.

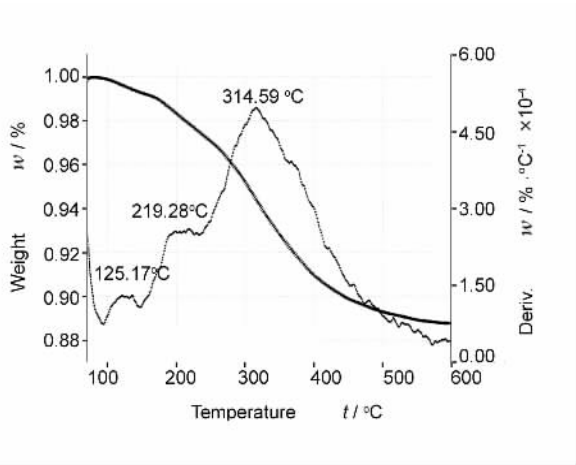


Fig. 2 TG curve of $\text{HNO}_3\text{-CH}_3\text{COOH-GIC}$ with a heating rate of $60\text{ }^\circ\text{C}/\text{min}$

On the basis of the reaction equations listed in references^[6-8], $\text{HNO}_3\text{-GIC}$, $\text{H}_2\text{SO}_4\text{-CH}_3\text{COOH-GIC}$, and $\text{HNO}_3\text{-CH}_3\text{COOH-GIC}$ can be expressed as: $[\text{graphite}^+ \cdot \text{HNO}_3 \cdot \text{NO}_3^-]_n$, $[\text{graphite}^+ \cdot \text{SO}_4^{2-} \cdot \text{CH}_3\text{COOH}]_n$, and $[\text{graphite}^+ \cdot \text{NO}_3^- \cdot \text{CH}_3\text{COOH}]_n$. In this study, nitric acid radical ion

and acetic acid molecule in $\text{HNO}_3\text{-CH}_3\text{COOH-GIC}$ are also contained in $\text{HNO}_3\text{-GIC}$ and $\text{H}_2\text{SO}_4\text{-CH}_3\text{COOH-GIC}$. So, thermal analysis of $\text{H}_2\text{SO}_4\text{-CH}_3\text{COOH-GIC}$ and $\text{HNO}_3\text{-GIC}$ were tested by the same heating rate as shown in Fig. 3.

Compared with the decomposition of $\text{H}_2\text{SO}_4\text{-GIC}$ as demonstrated in Fig. 1, the first decomposition peak of $\text{H}_2\text{SO}_4\text{-CH}_3\text{COOH-GIC}$ as observed in Fig. 3(a) corresponds to dehydration, and two smaller peaks are identified to correspond to the decomposition of SO_4^{2-} around $210\text{ }^\circ\text{C}$. The highest weight loss is observed between $300\text{ }^\circ\text{C}$ and $320\text{ }^\circ\text{C}$, which is not found in TG curve of $\text{H}_2\text{SO}_4\text{-GIC}$. As seen from material components to ternary expandable graphite that are synthesized, the content of CH_3COOH is more than that of HNO_3 or H_2SO_4 . It could be deduced that proportion of acetic acid molecule that is intercalated into graphite is more than the intercalation of other functional groups. Hereby, the maximal weight loss should have occurred due to the release of acetic acid, which is seen in TG curves of $\text{HNO}_3\text{-CH}_3\text{COOH-GIC}$ and $\text{H}_2\text{SO}_4\text{-CH}_3\text{COOH-GIC}$. As observed in Fig. 3(b), the first weight loss is attributed to the dehydration, and the subsequent to the release of NO_3^- , HNO_3 . On the basis of the above-mentioned information, it could be predicted that weight loss at $200\text{ }^\circ\text{C}$ corresponds to the loss of nitric acid radical ion, and the strongest peak at $350\text{ }^\circ\text{C}$ corresponds to the decomposition of HNO_3 . These results are also verified by infrared spectrograms of gas products.

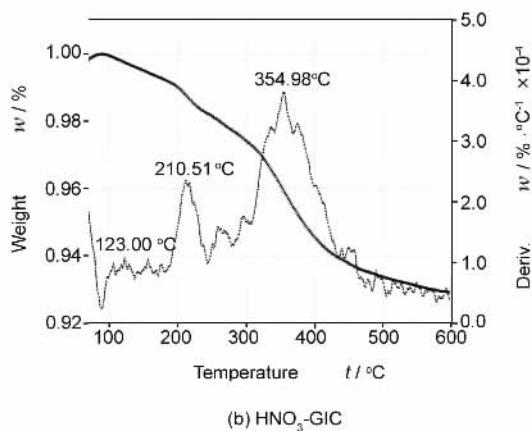
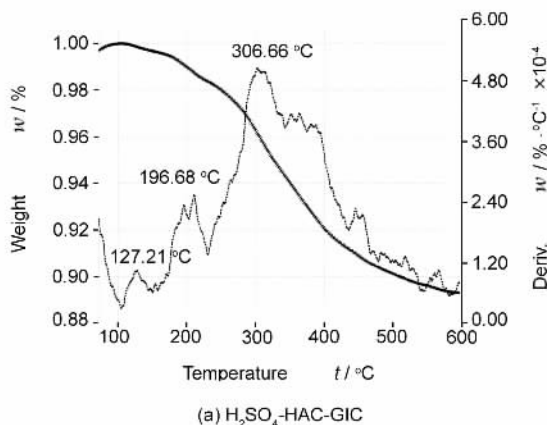


Fig. 3 TG curve s of $\text{HNO}_3\text{-GIC}$ and $\text{H}_2\text{SO}_4\text{-CH}_3\text{COOH-GIC}$ with a heating rate of $60\text{ }^\circ\text{C}/\text{min}$

Fig. 4 shows FTIR spectra of decomposition of $\text{HNO}_3\text{-CH}_3\text{COOH-GIC}$ heated to different temperatures. For $\text{HNO}_3\text{-CH}_3\text{COOH-GIC}$, there are two remarkable absorption peaks at 1430 and 840 cm^{-1} when expandable GIC is heated to $220\text{ }^\circ\text{C}$, which are characteristic peaks of nitric acid radical^[18]. It dem-

onstrates that the nitric acid radical ion escapes from graphite layers at ca. $220\text{ }^\circ\text{C}$. The O-H band of carboxyl stretching vibration, C=O band stretching vibration, and O-H band bending vibration are often used to identify carboxyl acid using infrared spectroscopy. A sharp peak corresponding to decomposition

spectra arises at $1\,710\text{ cm}^{-1}$ when the temperature of thermal analysis reaches $320\text{ }^{\circ}\text{C}$. Furthermore, vibration frequencies of C—H band, including asymmetrical and symmetrical bending, are located around $1\,470$ and $1\,380\text{ cm}^{-1}$, of which the latter is used to identify methyl structure. When —CH₃ is linked to other atoms, the peak will shift due to the change of bending constant. The stronger the electronegativity of the adjoining group is, the higher is the shift of wavenumber of the peak located at $1\,380\text{ cm}^{-1}$ ^[19]. As observed in Fig. 4, there is an absorption peak of the decomposition spectrum at $1\,410\text{ }^{\circ}\text{C}$. This results from the interaction of methyl and carboxyl groups. So, it is concluded that acetic acid molecule escapes from graphite layers when expandable graphite is heated to $320\text{ }^{\circ}\text{C}$, which is consistent with results from thermal analysis.

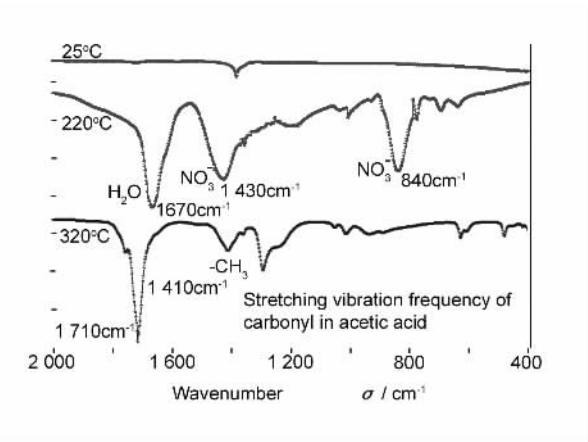


Fig. 4 FTIR spectra of decomposition of HNO₃-CH₃COOH-GIC heated to different temperatures

According to TG curves of H₂SO₄-GIC (Fig. 1) and HNO₃ - CH₃COOH - GIC (Fig. 5) at different

heating rates, the decomposition process and dynamical parameters are calculated according to Kissinger and Ozawa principles, as summarized in Tables 1 and 2.

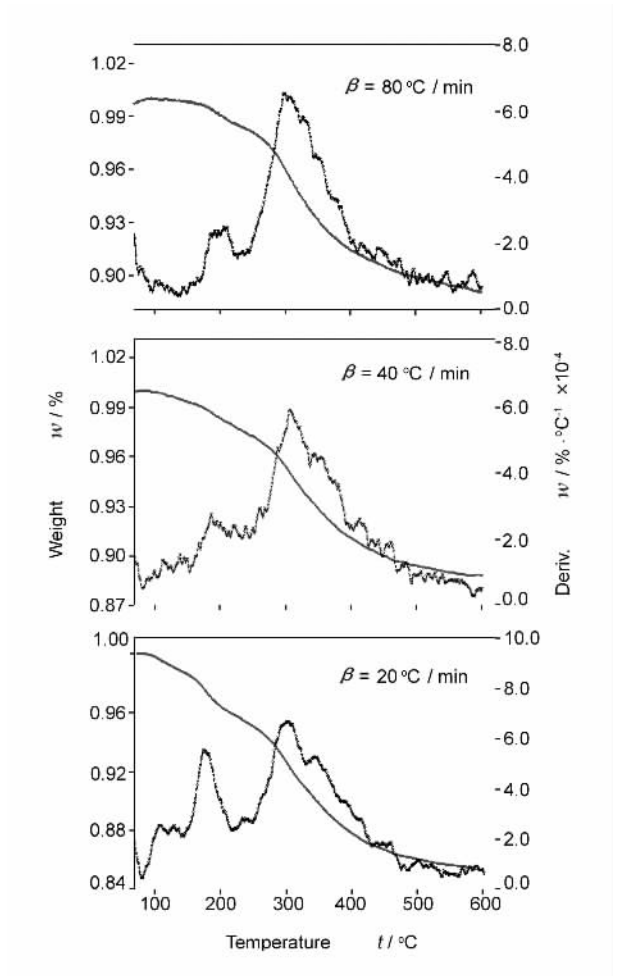


Fig. 5 TG curves of HNO₃-CH₃COOH-GIC at different heating rates

Table 1 Thermal decomposition of H₂SO₄-GIC and kinetics parameters

Peak	Peak temperature <i>t</i> / °C	Decomposition property and products	Kissinger law <i>E</i> / kJ · mol ⁻¹	Ozawa law lg <i>A</i>	Ozawa law <i>E</i> / kJ · mol ⁻¹
1st decomposition	247.4	Water and HSO ₄ ⁻ escaping from graphite layers	90.29	7.49	94.22
2nd decomposition	333.2	Sulfuric acid molecule escaping from expandable graphite			
3rd decomposition	456.9	Decomposition of residual compounds			

Table 2 Thermal decomposition of HNO₃-CH₃COOH-GIC and kinetics parameters

Peak	Peak temperature <i>t</i> / °C	Decomposition property and products	Kissinger law <i>E</i> / kJ · mol ⁻¹	Ozawa law lg <i>A</i>	Ozawa law <i>E</i> / kJ · mol ⁻¹
1st decomposition	208.4	Water and nitric acid radical ion escaping from graphite layers	91.23	8.73	94.14
2nd decomposition	315.6	Acetic acid molecule escaping from expandable graphite	114.80	8.94	118.2

4 Conclusions

In summary, the phase change and decomposition process of $\text{HNO}_3\text{-CH}_3\text{COOH-GIC}$, $\text{H}_2\text{SO}_4\text{-CH}_3\text{COOH-GIC}$, $\text{HNO}_3\text{-GIC}$, and $\text{H}_2\text{SO}_4\text{-GIC}$ were investigated by thermal analysis. By comparing TG curves of GICs, which contain similar groups, it was found that intercalated molecules, ions, and atoms escape from graphite layers. The absorbency spectra of decomposition products were in situ measured by the FTIR-associated TG apparatus. According to Kissinger and Ozawa principles, kinetics parameters of the exfoliation reactions are calculated. The main conclusions are as follows:

(1) NO_3^- and SO_4^{2-} escape from GIC at $200\text{ }^\circ\text{C}$ – $210\text{ }^\circ\text{C}$, HSO_4^- and H_2SO_4 escape at $240\text{ }^\circ\text{C}$ – $250\text{ }^\circ\text{C}$, and acetic acid molecule escapes from graphite layers at ca. $320\text{ }^\circ\text{C}$

(2) On the basis of the thermal analysis theory, the activation energy of the exfoliation reactions are evaluated, and it was found that they are all lower than 120 kJ/mol .

References

- [1] 康飞宇. 石墨层间化合物和膨胀石墨[J]. 新型炭材料, 2000, **15**(4): 80.
(KANG Fei-yu. Graphite intercalation compound and exfoliated graphite[J]. New Carbon Materials, 2000, **15**(4): 80.)
- [2] 稻垣道夫, 丰田义雄, 康飞宇, 等. 膨胀石墨的孔隙结构—中国国家自然科学基金和日本学术振兴会联合研究项目报道[J]. 新型炭材料, 2003, **18**(4): 241-249.
(Inagaki M, Toyoda M, KANG Fei-yu, et al. Pore structure of exfoliated graphite—A report on a joint research project under the scientific cooperation program between NSFC and JSPS[J]. New Carbon Materials, 2003, **18**(4): 241-249.)
- [3] 传秀云. 石墨层间化合物 GICs 的形成机理探讨[J]. 新型炭材料, 2000, **15**(1): 52-56.
(CHUAN Xiu-yun. Formation mechanisms of graphite intercalation compounds[J]. New Carbon Materials, 2000, **15**(1): 52-56.)
- [4] Toshiaki E, Masatsugu S, Morinobu E. Graphite Intercalation Compounds and Applications[M]. New York: Oxford University Press, 2003.
- [5] Chung D D L. Review graphite[J]. Journal of Material Science, 2002, **37**(5): 1475-1489.
- [6] 高林, 龚银香, 马玲. 膨胀次数对天然鳞片膨胀石墨微结构的影响[J]. 新型炭材料, 2006, **21**(3): 139-143.
(GAO Lin, GONG Yin-xiang, MA Ling. Effect of expansion time on the microstructure of an expanded natural flake graphite[J]. New Carbon Materials, 2006, **21**(3): 139-143.)
- [7] 高林, 马玲. 用柔性石墨制备低密度膨胀石墨块[J]. 新型炭材料, 2006, **21**(3): 253-258.
(GAO Lin, MA Ling. Preparation of low density monolithic expanded graphite from flexible graphite[J]. New Carbon Materials, 2006, **21**(3): 253-258.)
- [8] Celzard A, Maréché J F, Furdin G. Modelling of exfoliated graphite[J]. Process in Materials Science, 2005, **50**: 93-17.
- [9] 魏兴海, 张金喜, 史景利, 等. 无硫高倍膨胀石墨的制备及影响因素探讨[J]. 新型炭材料, 2004, **19**(1): 45-48.
(WEI Xing-hai, ZHANG Jin-xi, SHI Jing-li, et al. Preparation of sulfur-free highly expanded graphite[J]. New Carbon Materials, 2004, **19**(1): 45-48.)
- [10] 刘国钦, 闫珉. 利用细鳞片石墨制备膨胀石墨的研究[J]. 新型炭材料, 2002, **17**(2): 13-18.
(LIU Guo-qin, YAN Min. The preparation of expanded graphite using fine flaky graphite[J]. New Carbon Materials, 2002, **17**(2): 13-18.)
- [11] Inagaki M, Nakashima M, Soneda Y, et al. Room temperature exfoliation of graphite microgravity[J]. Carbon, 1993, **31**(8): 1349-1350.
- [12] Kuga Y, Oyama T, Wakabayashi T, et al. Laser-assisted exfoliation of potassium-ammonia-graphite intercalation compounds[J]. Carbon, 1993, **31**(1): 201-204.
- [13] Song Keming, Liu Jinpeng, Jin Tongshou et al. Preparation of sulfur-free and expandable graphite[J]. Journal of Inorganic Materials, 1997, **12**(2): 252-256.
- [14] 李冀辉, 黎梅, 扈海英, 等. 制备低硫可膨胀石墨的新方法[J]. 新型炭材料, 1999, **14**(1): 65-68.
(LI Ji-hui, LI Mei, HU Hai-ying, et al. A new preparation method of lower-sulfur content expandable graphite[J]. New Carbon Materials, 1999, **14**(1): 65-68.)
- [15] Kang F, Leng Y, Zhang T Y. Electrochemical synthesis and characterization of formic acid-graphite intercalation compounds[J]. Carbon, 1997, **35**(8): 1089-1096.
- [16] Shi Qizhen (Ed.). Thermoanalysis Kinetics and Thermokinetics[M]. Xi'an: Press of Science and Technology in Shanxi Province, 2001.
- [17] Hong Rongzu, Shi Qizhen. Thermoanalysis Kinetics[M]. Beijing: Press of Science, 2001.
- [18] Huang Deru, Wang Renqing (Ed.). Infrared and Raman Spectrum of Mineral and Coordination Compounds[M]. Beijing: Press of Chemistry Industry, 1997.
- [19] Li Runqing (Ed.). Spectral Analysis of Organic Structures[M]. Tianjin: Press of Tianjin University, 2002.

插层化合物在膨化过程中的热分解动力学

任 慧^{1,2}, 康飞宇¹, 焦清介², 崔庆忠²

(1. 清华大学 深圳研究生院, 广东 深圳 518055; 2. 北京理工大学 爆炸科学与技术国家重点实验室, 北京 100081)

摘 要: 采用红外傅立叶变换光谱仪与热重分析仪联动装置在线检测 $\text{HNO}_3\text{-CH}_3\text{COOH-GIC}$ 、 $\text{H}_2\text{SO}_4\text{-GIC}$ 及 $\text{H}_2\text{SO}_4\text{-CH}_3\text{COOH-GIC}$ 等插层石墨的相变及热分解过程, 同时通过快速扫描得到相应时间段内分解产物的红外光谱, 并运用 Kissinger-Ozawa 原理计算了几种典型膨化反应的动力学参数。研究结果揭示了膨化过程的热分解机理, 当升温速率在 $20\text{ }^\circ\text{C}/\text{min} \sim 80\text{ }^\circ\text{C}/\text{min}$ 范围时, 由实验数据计算出膨化反应表观活化能不大于 120 kJ/mol 。

关键词: 膨化; 热分解; 动力学; 插层

基金项目: 国家自然科学基金(50572047)

通讯作者: 康飞宇, E-mail: fykang@mail.tsinghua.edu.cn

作者简介: 任慧(1973-), 女, 山西阳泉人, 博士后, 讲师, 主要研究领域为纳米功能材料。E-mail: renhui@bit.edu.cn



久星导热油网

网站内容:

导热油资讯、导热油产品、供求信息、论文中心、俱乐部、化工 e 圈

E 时代久星特色服务:

1. 选择导热油时: 提供理化指标;
2. 设计系统时: 提供物性数据;
3. 用户需油时: 门对门服务;
4. 初用导热油时: 提供安全技术说明书;
5. 能耗上升时: 提供热油炉化学清洗剂并提供清洗方案;
6. 了解导热油时: 提供 130 页 15 万字鲍培编著的《导热油应用手册》;
7. 导热油应用时: 全程跟踪测试, 画出导热油使用曲线图, 找到最佳使用方案;
8. 系统生病时: 实施康复工程;
9. 接到求助时: 4 小时内提出解决方案, 在特殊情况下, 24 小时内赶扑现场;
10. 网络交流时: www.9xchem.com (久星导热油网) 能解答疑问;
11. 降低成本时: 提供导热油增寿剂、在线清洗剂、修复剂, 延长寿命 5~8 年;
12. 工艺更新时: 研制特种功能的导热油, 以满足用户需求。

上海久星公司生产经营久星从“心”开始:

导热油系列、导热油修复剂系列、导热油增寿剂、导热油在线清洗剂、热油炉清洗剂系列、电加热专用导热油、低温导热油($-50\text{ }^\circ\text{C}$)、道生导热油、橡胶行业专用导热油、食品行业专用导热油、锅炉燃料油、高温链条油系列等。久星牌—导热油”荣获 2006 年上海化工名优产品”。

上海久星化工有限公司

德国施罗德化工集团有限公司合作商

地址: 上海市茂兴路 96 号 (仁恒广场 2 座) 6G 邮编: 200127

总机: 021-22817772 22817773 短信网址: 编辑“导热油”到 50120

E-mail: bqp@9xchem.com jiuxingd@online.sh.cn